


6-2016

## Influencing Pathways that Cause Metastasis and Stemness in Epithelial Ovarian Cancer

Alyse Lynn Huiskens-Hill  
*California State University - San Bernardino*

Follow this and additional works at: <https://scholarworks.lib.csusb.edu/etd>

 Part of the [Biology Commons](#), [Cancer Biology Commons](#), [Cell Biology Commons](#), [Laboratory and Basic Science Research Commons](#), [Molecular Biology Commons](#), and the [Other Animal Sciences Commons](#)

---

### Recommended Citation

Huiskens-Hill, Alyse Lynn, "Influencing Pathways that Cause Metastasis and Stemness in Epithelial Ovarian Cancer" (2016). *Electronic Theses, Projects, and Dissertations*. 355.  
<https://scholarworks.lib.csusb.edu/etd/355>

This Thesis is brought to you for free and open access by the Office of Graduate Studies at CSUSB ScholarWorks. It has been accepted for inclusion in Electronic Theses, Projects, and Dissertations by an authorized administrator of CSUSB ScholarWorks. For more information, please contact [scholarworks@csusb.edu](mailto:scholarworks@csusb.edu).

INFLUENCING PATHWAYS THAT CAUSE METASTASIS AND  
STEMNESS IN EPITHELIAL OVARIAN CANCER

---

A Thesis  
Presented to the  
Faculty of  
California State University,  
San Bernardino

---

In Partial Fulfillment  
of the Requirements for the Degree  
Master of Science  
in  
Biology

---

by  
Alyse Lynn Huiskens-Hill

June 2016

INFLUENCING PATHWAYS THAT CAUSE METASTASIS AND  
STEMNESS IN EPITHELIAL OVARIAN CANCER

---

A Thesis  
Presented to the  
Faculty of  
California State University,  
San Bernardino

---

by  
Alyse Lynn Huiskens-Hill

June 2016

Approved by:

Nicole Bournias-Vardiabasis, Committee Chair, Biology

Jeffrey Thompson, Committee Member

Juli Unternaehrer, Committee Member

© 2016 Alyse Lynn Huiskens-Hill

## ABSTRACT

Ovarian cancer is the fifth leading cause of cancer death in women between the ages of 35 and 74. With 22 thousand new cases and 15 thousand deaths annually ovarian cancer is among the most deadly cancers with a death to incidence ratio of 68%. With 70% of cases High Grade Serous Ovarian Carcinoma (HGSOC) is the most common type of ovarian cancer and causes 90% of ovarian cancer deaths. 80% of patients have reoccurrence within five years and only 15-30% of patients with recurrent metastatic ovarian cancer respond to current therapies, chemotherapy and surgery. One reason for the high reoccurrence rate is thought to be linked to the heterogeneity of tumors: there is evidence that, among tumor cells, a subpopulation is cancer stem cells (CSCs). Since CSCs are frequently drug resistant, when the patient undergoes chemotherapy many of the cells may die but the CSCs are left behind and the tumors can therefore regrow. CSCs are also more likely to undergo epithelial-mesenchymal transition which gives these cells the ability to more readily migrate and invade through the extracellular matrix, leaving the primary tumor to form metastases. One key inducer of EMT and therefore possibly of metastasis of particular interest in this project is SNAI1 (Snail). It is therefore the goal of this project to understand the growth, makeup and metastatic ability of HGSOC cell lines to test possible strategies to decrease growth of cancer and prevent metastasis.

In this thesis project the phenotype, CSC population make up, and functionality of various HGSOC cell lines was examined. The cell lines assessed were A2780, Kuramochi, OVSAHO, COV318, SKOV3 and OVCAR8. A Snail knockdown OVCAR8 cell line was also assessed as described above and in a xenograft model. It was determined that the cell lines show varying phenotype from epithelial like to mesenchymal like morphology and the cell lines have varying concentrations of cancer stem cells. It was also determined that the CSC population of the HGSOC cell lines were positive for both epithelial and mesenchymal markers in the same cells. OVCAR8 stood out as a hybrid line with both epithelial and mesenchymal characteristics and was therefore chosen for the Snail knockdown model. In the Snail knockdown we observed that CSC markers were reduced, however no change between control and knockdown was seen in the *in vitro* functional experiments. There was a difference seen between Snail knockdown and control in the *in vivo* mouse xenograft model. Snail knockdown showed a trend for decreasing tumor burden in both primary and metastatic tumors and showed a significant decrease in growth of metastatic tumor at day 43. Based on these results Snail may be an important target for cancer therapy.

## ACKNOWLEDGEMENTS

Firstly, I would like to acknowledge Dr. Juli Unternaehrer for allowing me to work on this project in her laboratory and thank her for the incredible guidance I received throughout my time on this thesis project. I would also like to acknowledge the individuals in the Unternaehrer lab who helped with the progress leading to the completion of this thesis project, Linda Sanderman, Hugo Campos, Michael McCarthy, Hanmin Wang, and Evgeny Chirshev. I would like to acknowledge and thank Dr. Nicole Bournias-Vardiabasis and Dr. Jeffrey Thompson for all of their help serving on my thesis committee. I would also like to acknowledge the CIRM Bridges program and Loma Linda University for the funding that allowed this project to be undertaken. Last, I would like to thank and acknowledge my wonderful husband Christopher Hill and family who are always so supportive of me.

## TABLE OF CONTENTS

ABSTRACT .....	iii
ACKNOWLEDGEMENTS.....	v
LIST OF TABLES .....	viii
LIST OF FIGURES .....	ix
CHAPTER ONE: INTRODUCTION	
1.1 Epithelial Mesenchymal Transition.....	1
1.2 Epithelial Ovarian Cancer .....	2
1.3 Cancer Stem Cells .....	3
1.4 The Importance of the Let-7 and Snail Interaction .....	5
1.5 Working Hypothesis .....	6
Aim1: Characterization of Epithelial Ovarian Cancer Cell Lines for Epithelial Mesenchymal Transition Status, Cancer Stem Cell Makeup, and Metastatic Potential .....	7
Aim 2: Characterization of Snail Inhibition Model of Epithelial Ovarian Cancer for Epithelial Mesenchymal Transition Status, Cancer Stem Cell Makeup, and Metastatic Potential .....	7
CHAPTER TWO: MATERIALS AND METHODS	
2.1 Cell Culture – <i>In vitro</i> Assays	
2.1.1 Ovarian Cancer Cell Culture .....	9
2.1.2 Motility .....	9
2.1.3 Anchorage Independent Growth .....	10
2.2 Xenograft – <i>In vivo</i> Assays	
2.2.1 Preparation of Ovarian Cancer Cells.....	11
2.2.2 Lentiviral Knockdown .....	12



2.2.3 Surgical Orthotopic Injection of Ovarian Cancer Cells .....	13
2.2.4 Live Mouse Imaging .....	13
2.2.5 Tumor Harvest .....	13
2.3 Molecular Biology	
2.3.1 RNA Extraction and qPCR .....	14
2.3.2 Flow Cytometry .....	15
CHAPTER THREE: RESULTS	
3.1 Aim 1: The Characterization of Epithelial Ovarian Cancer Cell Lines for Epithelial Mesenchymal Transition Status, Cancer Stem Cell Makeup, and Metastatic Potential	
3.1.1 Epithelial Mesenchymal Transition Status and Cancer Stem Cell Makeup of Epithelial Ovarian Cancer Cell Lines.....	17
3.1.2 Metastatic Potential of Epithelial Ovarian Cancer Cell Lines	23
3.2 Aim 2: The Effect of Snail Knockdown on Epithelial Mesenchymal Transition Status, Cancer Stem Cell Makeup, and Metastatic Potential of an Epithelial Ovarian Cancer Cell Line OVCAR8	
3.2.1 Confirmation of Snail Knockdown .....	24
3.2.2 Epithelial Mesenchymal Transition Status and Cancer Stem Cell Makeup of Snail Knockdown Model.....	26
3.2.3 Metastatic Potential in Snail Knockdown Model.....	28
3.2.4 Orthotopic Xenograft of Snail Knockdown OVCAR8 .....	29
CHAPTER FOUR: DISCUSSION	
Epithelial Mesenchymal Transition and Cancer Stem Cells in Epithelial Ovarian Cancer.....	31
Epithelial Mesenchymal Transition and Cancer Stem Cells in Snail Knockdown Model of Epithelial Ovarian Cancer .....	33
REFERENCES .....	36

## LIST OF TABLES

Table 1. Primer sequences used for qPCR .....	14
Table 2. Antibodies used for flow cytometry .....	15

## LIST OF FIGURES

Figure 1. Overview of epithelial mesenchymal transition.....	1
Figure 2. Overview of cancer stem cell theory leading to cancer relapse.....	4
Figure 3. Schematic representation of the Snail/Let-7 and Snail/cadherin interactions. ....	6
Figure 4. Schematic representation of the hypothesis.....	7
Figure 5. Luciferase plasmid construct. ....	12
Figure 6. Flow cytometry gating with the aid of isotype stained population .....	16
Figure 7. Phase contrast brightfield microscopy images of epithelial ovarian cancer cell lines.....	18
Figure 8. Epithelial mesenchymal transition markers in epithelial ovarian cancer cell lines.....	19
Figure 9. Cancer stem cell markers in epithelial ovarian cancer cell lines.....	21
Figure 10. Cancer stem cells and epithelial mesenchymal transition .....	22
Figure 11. Metastatic potential assays of epithelial ovarian cancer .....	24
Figure 12. Confirmation of Snail knockdown and let-7 expression in shSnail....	25
Figure 13. Epithelial mesenchymal transition markers in Snail knockdown model.....	26
Figure 14. Cancer stem cell markers in Snail knockdown model.....	28
Figure 15. Metastatic potential assays of Snail knockdown epithelial ovarian cancer.....	29
Figure 16. Xenograft model of Snail knockdown epithelial ovarian cancer.....	30

## CHAPTER ONE

### INTRODUCTION

#### 1.1 Epithelial Mesenchymal Transition

Epithelial-mesenchymal transition (EMT) is the process by which an epithelial cell becomes mesenchymal and gains the ability to exit the epithelial layer of cells and invade through the basement membrane layer. EMT can occur as the result of many cellular pathways including Wnt, Nodal, FGF, BMP, and Notch pathways<sup>1</sup>. EMT events normally occur during embryonic development. These developmental events that utilize EMT include embryo implantation, gastrulation, and neural crest formation<sup>2</sup>.

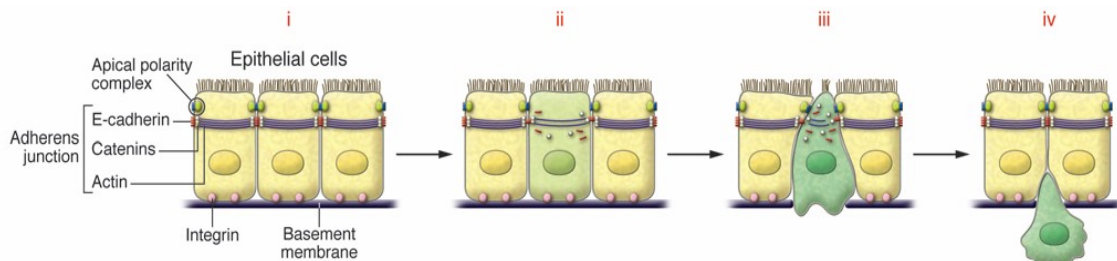


Figure 1. Overview of epithelial mesenchymal transition<sup>2</sup>.

In cancer, EMT events lead to an invasive and metastatic phenotype allowing cells to leave the primary tumor and invade secondary sites forming metastasis<sup>2</sup>. EMT can be observed through changes in transcription factors and

proteins involved in EMT pathways. Some of the factors important in this process are Snail (Snai1), E-cadherin, and N-cadherin. Snail and other transcription factors are one controlling step in EMT. Snail has the ability to repress the transcription of E-cadherin, an adherens junction protein important for epithelial phenotype, and other epithelial proteins<sup>3</sup>. With this loss of E-cadherin there is a switch to N-cadherin production in the mesenchymal phenotype<sup>4</sup>. Not only is Snail involved in the EMT process it has also been linked to the development of chemoresistance in cancer linked to an increase in stemness<sup>5,6</sup>.

## 1.2 Epithelial Ovarian Cancer

Ovarian cancer is the fifth leading cause of cancer death in women<sup>7</sup>. With 22,000 new cases and 15,000 deaths annually in the US, ovarian cancer has the highest death to incidence ratio of any gynecologic cancer<sup>8</sup>. Epithelial ovarian cancer (EOC) develops in the epithelial layer of the ovary and most patients are diagnosed in late stages. About three quarters of ovarian cancer patients present with stage III or IV tumors<sup>9</sup>, which means the diseased cells are in a highly aggressive state and have metastasized within the peritoneal cavity either by direct extension from the ovary or through the seeding of the cavity by the production of ascites<sup>10</sup>. With 70% of cases, High Grade Serous Ovarian Carcinoma (HGSOC) is the most common type of ovarian cancer and causes 9 out of 10 of ovarian cancer deaths. About 70% of epithelial ovarian cancer patients experience relapse<sup>11</sup> and only 15-30% of patients with recurrent

metastatic ovarian cancer respond to current therapies of chemotherapy and tumor debulking surgery<sup>12</sup>.

### 1.3 Cancer Stem Cells

Tumors are a heterogeneous mixture of cell types<sup>13</sup>. Cancer Stem Cells (CSCs), also known as tumor initiating (TI) cells, are one of these cell types. CSCs are thought to be more readily able to leave a primary tumor and invade a secondary site (undergo metastasis). Circulating tumor cells (CTCs) in patients have been identified in many cancers to have CSC and EMT markers<sup>14</sup>; this has not yet been reported in ovarian cancer. CSCs are also believed to play a role in drug resistance in cancer due to the fact that after chemotherapy many cancers return<sup>15</sup>. This role of chemoresistance of CSCs has been confirmed in ovarian cancer<sup>16,17</sup>. Like normal stem cells CSCs possess self-renewal capacity shown by the ability of isolated CSC populations to recapitulate the cancer tumor phenotype *in vivo*<sup>16</sup>. Because of this ability combined with the ability of CSCs to evade traditional cancer therapies, relapse occurs if CSCs are left behind after treatment.

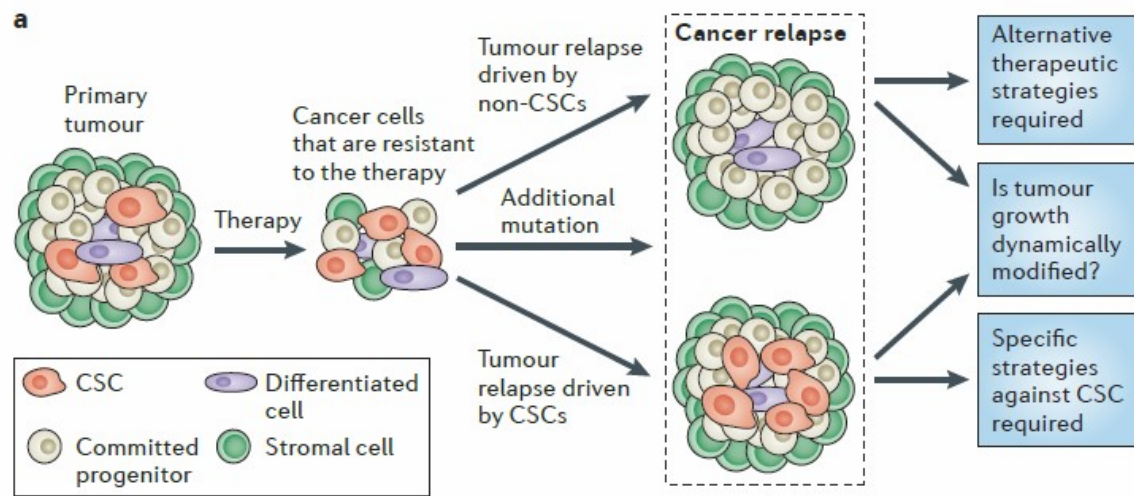


Figure 2. Overview of cancer stem cell theory leading to cancer relapse<sup>18</sup>.

Cancer Stem cell make up of a population can be determined by looking at the presence of ribonucleic acids (RNAs) that mark pluripotency such as Nanog, Lin28, and Oct4<sup>19</sup>. The presence of these stem cell markers are indicative of pluripotency, as opposed to multipotency as might be predicted for tissue stem cells. Lin28 has been shown to be highly expressed in some brain tumors, and knockdown of Lin28 in these tumors decreased the expression of Nanog and Oct4<sup>20</sup>, therefore the expression of these pluripotency related RNAs is very important in assessing a stem cell phenotype. There is some controversy as to which markers best define ovarian CSC populations<sup>13</sup>. There is also some debate on what constitutes a progenitor cancer cell versus a CSC; it was therefore important for this study to access many of these markers and have a strict definition of what was identified as a CSC population. Ovarian CSC

populations can also be identified in a cell population through the use of Flow Cytometry for known ovarian CSC markers CD44, CD133, CD117 (c-kit), and Aldehyde Dehydrogenase 1.<sup>13,21</sup> Cancer cell lines with larger populations of cancer stem cells should be more readily metastatic. Cells with more metastatic ability have more activity in functional assays such as the scratch assay for motility analysis and the soft agar assay for anchorage independent growth ability.

#### 1.4 The Importance of the Let-7 and Snail Interaction

Snail, which is known to cause EMT by repressing E-cadherin and other epithelial gene expression, has been shown to inhibit the microRNA Let-7<sup>22</sup>. Let-7 promotes differentiation and inhibits self-renewal via its targets including HMGA2, LIN28, IMP-1, CDC34, and many others<sup>23</sup>. Let-7 is also seen as a tumor suppressor due to its repression of targets such as c-Myc and Ras<sup>24</sup>. Because of this relationship between Let-7 and Snail, Let-7 and pluripotency, and the involvement of Snail in the EMT process, Snail could be a very important target in cancer research.



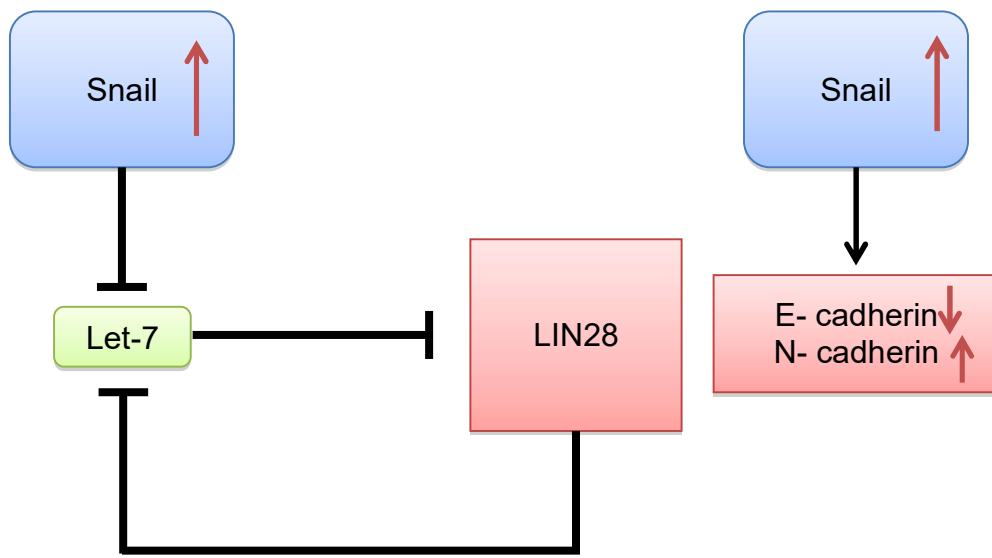


Figure 3. Schematic representation of the Snail/Let-7 and Snail/cadherin interactions. Snail up-regulation leads to Let-7 down regulation and increased stemness of cells. Figure adapted from Unternaehrer et.al.<sup>22</sup>

### 1.5 Working Hypothesis

Because Snail is involved in promotion of EMT and in Let-7 inhibition, if we inhibit Snail we can inhibit EMT and metastasis, and promote tumor suppression. We should therefore see a shift in EMT status, CSC makeup, and metastatic potential with knockdown of Snail.

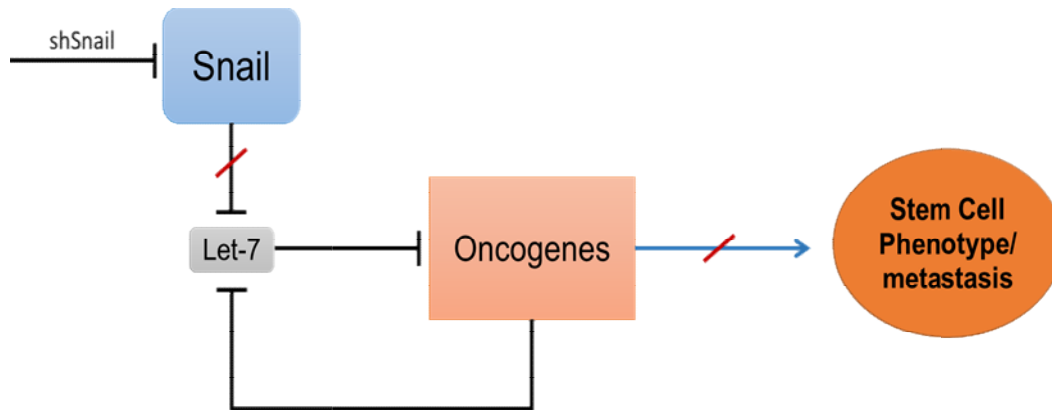


Figure 4. Schematic representation of the hypothesis.

Aim 1: Characterization of epithelial ovarian cancer cell lines for Epithelial Mesenchymal Transition status, Cancer Stem Cell makeup, and metastatic potential

Epithelial ovarian cancer cell lines A2780, Kuramochi, OVSAHO, COV318, SKOV3, and OVCAR8 were analyzed by qPCR at the level of RNA for EMT and CSC markers. EOC cell lines were analyzed with flow cytometry for EMT and CSC markers. Finally, EOC cell lines were analyzed with Scratch and Soft-agar assays to determine the relative metastatic potential of the lines.

Aim 2: Characterization of Snail inhibition model of epithelial ovarian cancer for Epithelial Mesenchymal Transition status, Cancer Stem Cell makeup, and metastatic potential

Epithelial ovarian cancer cell line OVCAR8 Snail knockdown and control cell lines were analyzed with qPCR at the level of RNA for EMT and CSC markers. Knockdown and control cell lines were analyzed with flow cytometry for EMT and CSC markers. Knockdown and control cell lines were then analyzed

with scratch and soft-agar assays to determine the relative metastatic potential of the lines. Finally, knockdown and control cell lines are used in a xenograft model to determine *in vivo* primary and metastatic growth.

## CHAPTER TWO

### MATERIALS AND METHODS

#### 2.1 Cell Culture – *In vitro* Assays

##### 2.1.1 Ovarian Cancer Cell Culture

Human High Grade Serous Ovarian Carcinoma cell lines were used for all experiments. The cell lines used were A2780, Kuramochi, OVSAHO, COV318, SKOV3, and OVCAR8. A fibroblast line, D2F, was also used as a control in some experiments. A2780, OVSAHO, SKOV3, OVCAR8 and D2F cells were cultured in Dulbecco's Modification of Eagle's Medium (DMEM) with 10% fetal bovine serum (FBS), 1% penicillin-streptomycin (PS), and 1% L-Glutamine (L-Glut). COV318 cells were cultured in DMEM with 10%FBS, 1% PS, 1% L-Glut, and 1% antibiotic-antimycotic (anti-anti). Kuramochi were cultured in Roswell Park Memorial Institute Medium (RPMI) with 10% FBS, 1% anti-anti, 1% L-Glut, human insulin 0.25U/ml, and 1x MEM non-essential amino acids (NEAA). Images were taken of each cell line with a bright field microscope with phase contrast to assess general morphology of the cell lines.

##### 2.1.2 Motility

To access motility of cell lines, a scratch wound healing assay was performed. Cells were grown to 90%+ confluency in 24-well tissue culture plates with ibidi inserts for wound closure assay (Culture-Inserts for self-insertion Catalog# 80209). Cells were plated and wounds imaged in triplicate. Images of wounds were taken every 4 hours for a 24-hour period after removal of insert

with a bright field microscope with phase contrast. Images were assessed with imageJ to measure size of wound. Six measurements of the wound width were taken for each image at each four-hour time point and averaged per well. Wound sizes were averaged for each cell line and compared through time lapse.

### 2.1.3 Anchorage Independent Growth

Soft agar assay was performed to assess the cell lines for ability to grow and form colonies in an anchorage independent growth environment, an ability which is a hallmark of aggressive cancer cells. Six-well plates were prepared with a bottom layer of Noble agar and DMEM Media mix. The noble agar was prepared as a 7% solution and was heated to mix agar powder with sterile distilled water. DMEM powder was mixed with sterile distilled water to make a 2x concentration of DMEM and was mixed with 20% FBS, 2% PS, 2% L-Glut, and 2% anti-anti. The 2x DMEM mixture and the 7% agar were mixed together at a one to one ratio at 42°C and 1mL of the mixture was added into each well of all 6-well plates to be used. This layer is allowed to cool at 37°C for at least one hour. Final concentration of this bottom agar layer was 1x DMEM mixture and 3.5% agar. The next agar layer was then prepared using 3% noble agar heated to mix powder with water. DMEM was prepared by diluting the 2x DMEM to 1x and adding 10% FBS, 1% PS, 1% L-Glut, and 1% anti-anti. Cells were then added at a concentration of 100,000 cells per milliliter in to the 1x DMEM mixture. The 3% agar was allowed to cool to 42°C then mixed with the DMEM cell mixture at a one to one ratio. 1mL of this mixture was then added on top of the first agar

layer in each well of the 6-well plates. The final concentrations in this layer were 1.5% agar, 0.5x DMEM mixture, and 50,000 cells per well. This layer was allowed to cool at 37°C for at least one hour. After cooling a 0.5 mL feeding layer was added to the top of the agar wells, the feeding layer consists of 1x DMEM, 10% FBS, 1%PS, 1% L-Glut, and 1% anti-anti. Cells were allowed to grow for 30 days and were fed at least twice per week with 0.5 mL feeding media per well. Wells were stained with 0.01% crystal violet at 37°C for 30 minutes and washed with water until colonies could be seen and counted with the naked eye.

## 2.2 Xenograft – *In vivo* Assays

### 2.2.1 Preparation of Ovarian Cancer Cells

To allow *in vivo* visualization, cells were virally transduced with a luciferase/GFP expression vector. Luciferin was added to cells or mice to allow bioluminescence imaging; plasmid design shown in Figure 4. The cells were then selected for and isolated by their fluorescence through the use of a FACS Aria flow cytometry cell sorter at the Genomics Core at the University of California Riverside.

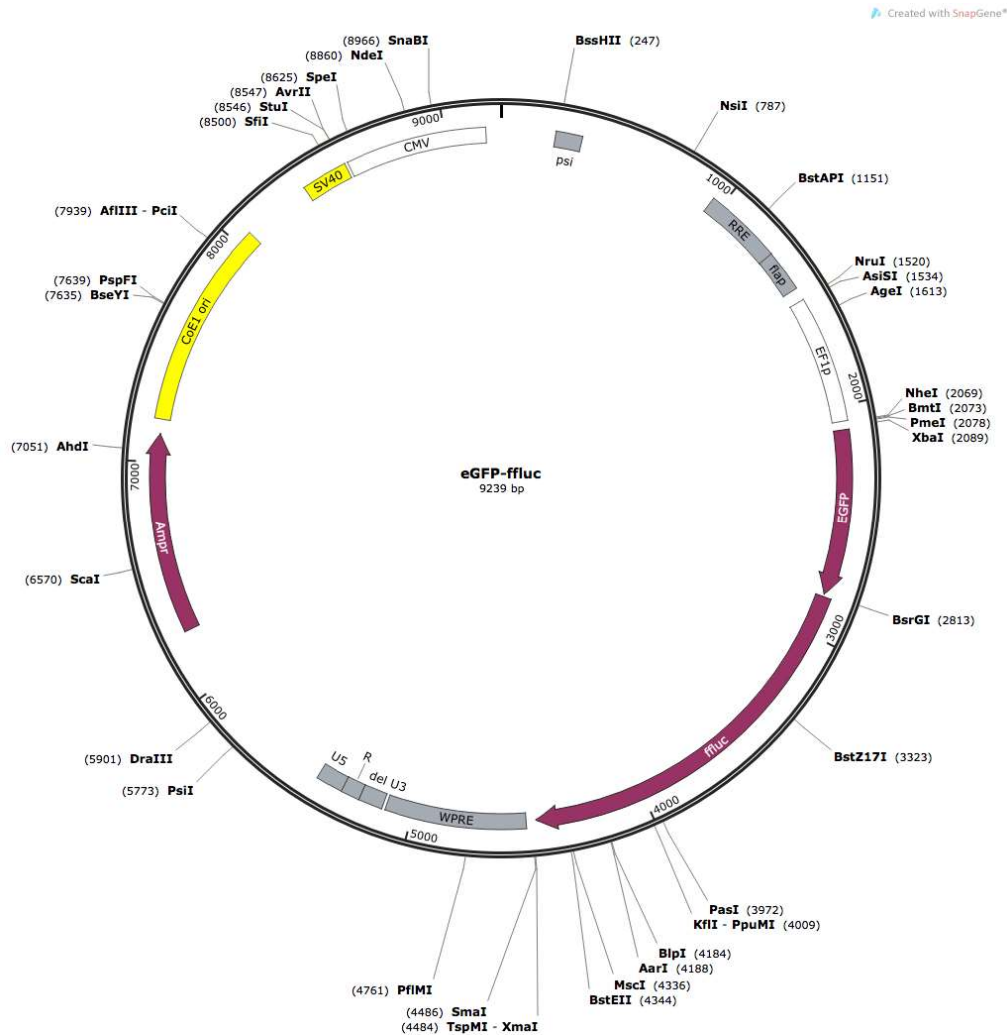


Figure 5. Luciferase plasmid construct.

## 2.2.2 Lentiviral Knockdown

Snail or control (scrambled) knockdown (KD) cells were utilized for xenograft experiments<sup>22</sup>. Stable cell lines with pLK0.1-based small hairpin (sh) RNA vectors were created by selection with puromycin. Cells were then cultured in order to obtain the number of cells to be injected during surgery.

### 2.2.3 Surgical Orthotopic Injection of Ovarian Cancer Cells

The ovarian cancer cells were prepared at  $2.5 \times 10^5$  cells per mouse in phosphate-buffered saline (PBS) and ovarian bursa injections were done as follows: before injection the cells were mixed with equal parts Matrigel from Corning (catalog #354248). The mouse was anesthetized and the right ovarian bursa was exposed through a dorsal incision. The cells were injected into the ovarian bursa, the bursa was replaced in the mouse, and the incision was closed. The mice were monitored for post-surgical recovery twice daily for three days, then daily for four days.

### 2.2.4 Live Mouse Imaging

Mice were imaged 1-2x weekly with an IVIS Lumina Series III *In Vivo* imaging system by PerkinElmer. Mice were anesthetized and given an intraperitoneal injection of luciferin. Images of mice were analyzed using Living Image *In Vivo* Imaging Software to determine size of primary and metastatic tumors. At the time of imaging weights and girth of mice were recorded.

### 2.2.5 Tumor Harvest

Mice were euthanized according to a Loma Linda University Institutional Animal Care and Use Committee approved protocol. Necropsy was then performed, removal of tumors from mouse with pictures and notes on location of tumor were done. Tumors are weighed and then processed for further assessment. A portion of each primary tumor or metastasis was sent to histology for further analysis. The remaining tumor was finely chopped and a portion was



saved for RNA analysis through qPCR. The remainder of the tumor is then broken down to the cellular level by washing the chopped tumor through a basket filter and cells were collected and saved for flow cytometry and western blot analysis.

## 2.3 Molecular Biology

### 2.3.1 RNA Extraction and qPCR

RNA extraction was performed using TRIzol Reagent (catalog #15596) from Life Technologies. CDNA preparation was performed in MultiGene OptiMax by Labnet International, Inc. using Maxima First Strand cDNA Synthesis Kit (catalog #K1671) by Thermo Scientific. Quantitative PCR was performed using KAPA SYBR FAST qPCR Kit Master Mix (2x) Universal (catalog #KK4600) in a Stratagene Mx3005P by Agilent Technologies. Primers used for cancer stem cell analysis included human Nanog, Lin28, and Oct4. Primers used for epithelial to mesenchymal phenotype included human E-cadherin, N-cadherin, and Snail. Actin $\beta$  was used as a control for all primers. All primers were purchased from Integrated DNA Technologies (IDT).

Table 1. Primer sequences used for qPCR.

Primer for	Forward	Reverse
Nanog	5'-CAAAGGCAAACAACCCACTT-3'	5'-TCTGCTGGAGGCTGAGGTAT-3'
Lin28	5'-GAGCATGCAGAAGCGCAGATCAAA-3'	5'-TATGGCTGATGCTCTGGCAGAAAGT-3'
Oct4	5'-AAGCGATCAAGCAGCGACTAT-3'	GGAAAGGGACCGAGGAGTACA-3'
E-cadherin	5'-TGCCCAGAAAATGAAAAAGG-3'	5'-GTGTATGTGGCAATGCGTTC-3'
N-cadherin	5'-GAGGAGTCAGTGAAGGAGTCA-3'	5'-GGGAAGTTGATTGGAGGGATG-3'
Snail	5'-CACTATGCCGCGCTCTTTC-3'	5'-GGTCGTAGGGCTGCTGGAA-3'
ActB	5'-TGAAGTGTGACGTGGACATC-3'	5'-GGAGGAGCAATGATCTTGAT-3'

### 2.3.2 Flow Cytometry

Flow cytometry analysis was performed on cell line and mouse xenograft samples. Cells were preserved in FACS Stain made of PBS with 1% FBS, 0.1% Sodium Azide, and 2mM EDTA. Cells were stained in FACS stain with antibodies at 4°C for 15 minutes, washed, and then fixed in FACS Fix, FACS Stain + 1% PFA. UltraComp eBeads (catalog #01-2222) from affymetrix eBioscience were used for compensation and were stained as single stain samples. Flow cytometry was performed on MACSQuant Analyzer 10 by Miltenyi Biotec and analysis of data was performed using FlowJo Version 10 from FLOWJo, LLC. Antibodies for CD44, CD117 (c-Kit), and CD133, as well as “Aldefluor” a fluorescent reagent system to detect aldehyde dehydrogenase 1 (ALDH1) were used to analyze cancer stem cell makeup of the cell population. Antibodies for E-cadherin (CD324) and N-cadherin (CD325) were used to analyze epithelial or mesenchymal makeup of the cell population. Populations were gated with the use of isotypes: each antibody channel was gated separately against forward scatter then overlaid to determine populations positive for multiple antibodies as shown in Figure 6.

Table 2. Antibodies used for flow cytometry.

Antibody/Kit	Source	Clone	Manufacture	Catalog #	Isotype	Catalog #
CD44	Mouse	G44-26	BD Biosciences	561292	IgG <sub>2b</sub> ,k	560374
CD117	Mouse	A3C6E2	Miltenyi Biotec	130-099-326	IgG1, k	130-100-098
CD133	Mouse	293C3	Miltenyi Biotec	130-090-854	IgG <sub>2b</sub> ,k	400319
E-cadherin	Rat	67A4	Miltenyi Biotec	130-099-141	IgG1	130-098-563
N-cadherin	Mouse	8C11	BD Biosciences	563435	IgG1, k	550795
Aldefluor	N/A	N/A	Stemcell Technologies	01700	Control in kit	

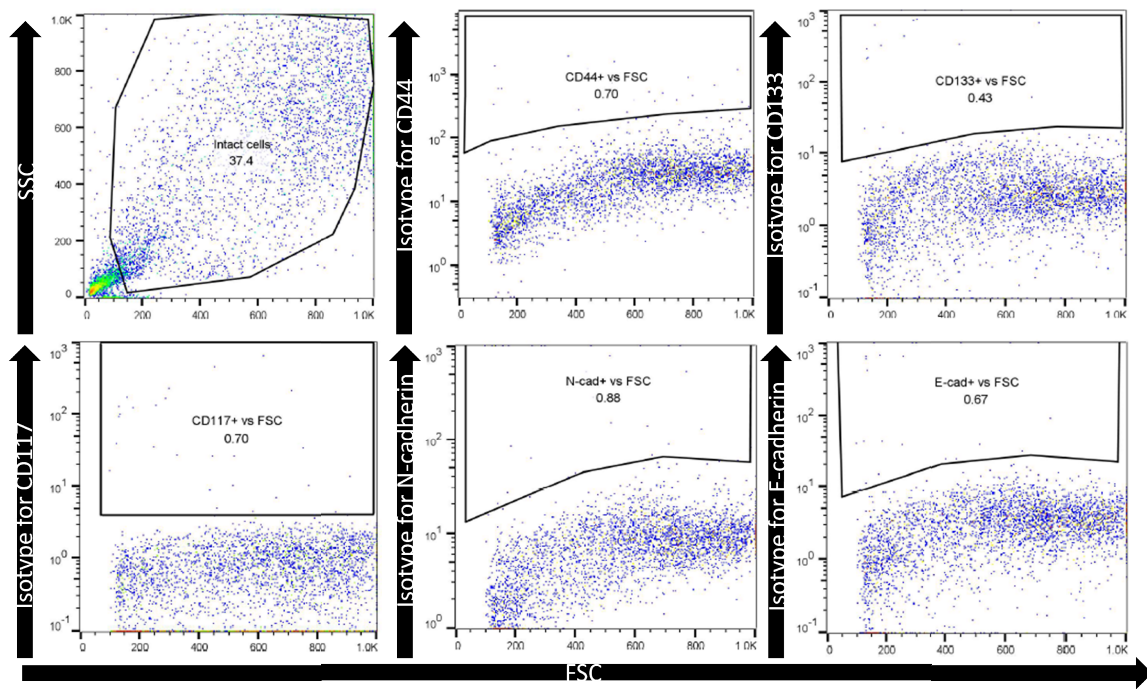


Figure 6. Flow cytometry gating with the aid of isotype stained population.

## CHAPTER THREE

### RESULTS

#### 3.1 Aim 1: The Characterization of Epithelial Ovarian Cancer Cell Lines for Epithelial Mesenchymal Transition status, Cancer Stem Cell makeup, and metastatic potential

##### 3.1.1 Epithelial Mesenchymal Transition Status and Cancer Stem Cell Makeup of Epithelial Ovarian Cancer Cell Lines

EOC cell lines were analyzed based on appearance in phase contrast bright field microscopy to determine general morphology and ability of cell lines to form colony like structures (Figure 7). It was determined by appearance and ability to form colony like structures that Kuramochi and OVSAHO have the most epithelial morphology. It was determined SKOV3 and COV318 have a more mesenchymal morphology. Based on their less epithelial structure but retention of the colony forming ability A2780-luc and OVCAR8 appear to be somewhat mesenchymal and somewhat epithelial.

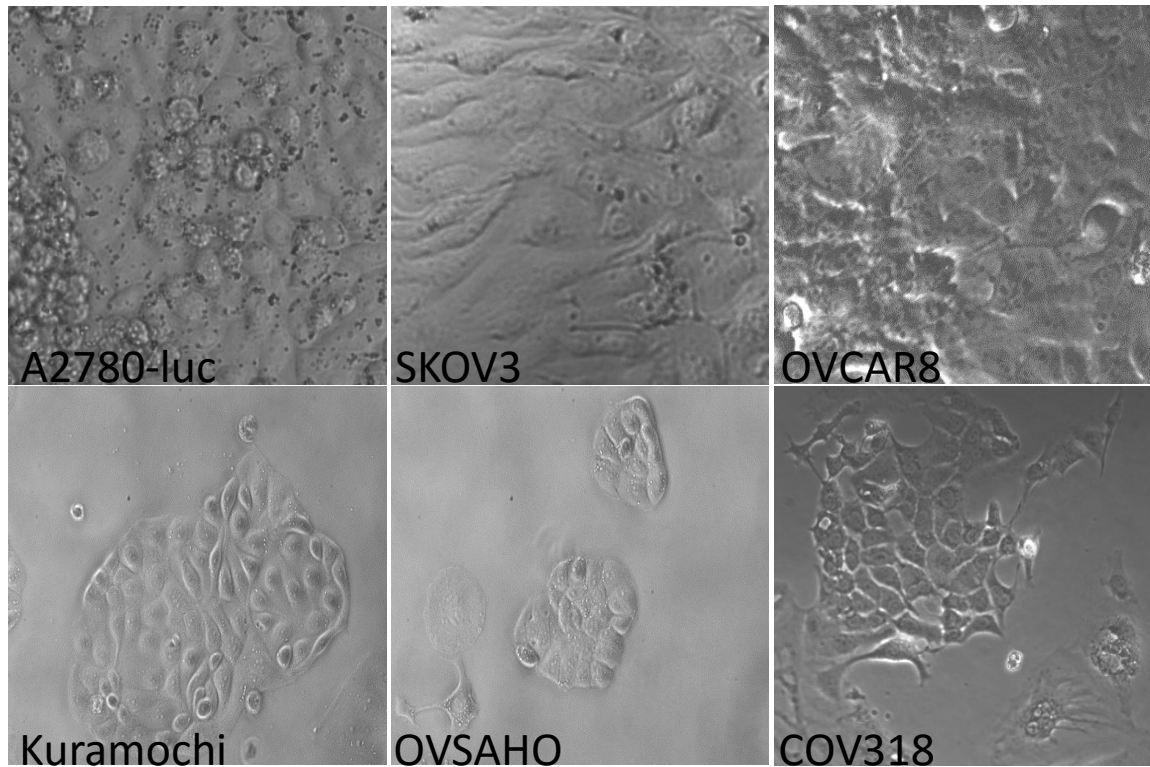


Figure 7. Phase contrast bright field microscopy images of epithelial ovarian cancer cell lines.

With the use of qPCR of Snail, N-cadherin, and E-cadherin the cell lines can be identified as having epithelial or mesenchymal mRNA expression. If the E-cadherin expression is high and the N-cadherin is low the cells can be identified as more epithelial than mesenchymal. Therefore, OVCAR8, and OVSAHO can be identified as having epithelial mRNA expression and COV318 and SKOV3 can be identified as having mesenchymal mRNA expression (Figure 8a). Flow cytometry showed the protein level of E-cadherin was high in all the EOC cell lines (Figure 8b). The cell lines were split into two groups based on having larger N-cadherin populations: COV318, SKOV3 and OVCAR8 were all

designated as mesenchymal-like, and having a smaller N-cadherin population. A2780-luc and Kuramochi were classified as epithelial. It was also observed that many cells were double positive for E-cadherin and N-cadherin.

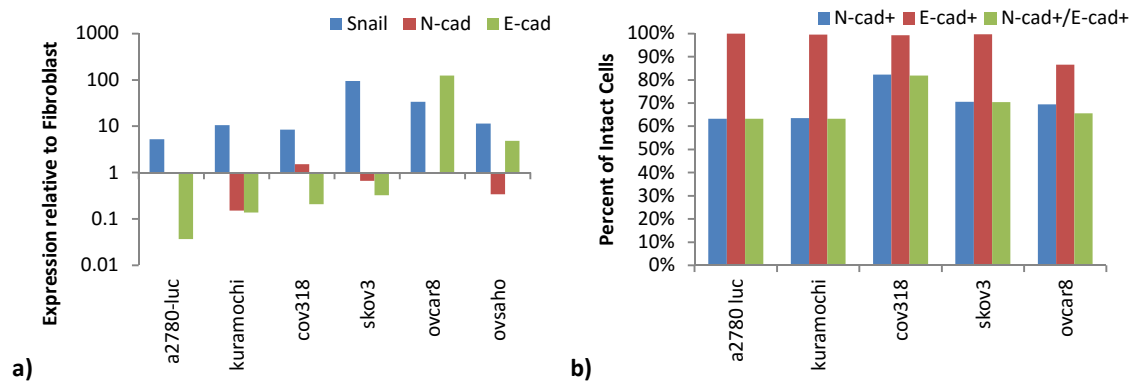


Figure 8. Epithelial mesenchymal transition markers in epithelial ovarian cancer cell lines. a) qPCR for Snail, N-cadherin, and E-cadherin expression in EOC cell lines. b) Flow cytometry percent positive cells for E-cadherin, N-cadherin, and E- and N-cadherin double positive cells.

The CSC and pluripotency marker Lin28 is detectable in all cell lines except COV318 and the marker Nanog has detectable expression in COV318 and OVSAHO (Figure 9a); Oct4 expression was low in all cells. The high Lin28 levels in comparison to fibroblasts could be explained by the lower let-7 miRNA levels observed in the cell lines (Figure 9b). CD44 positive populations range from 6 to 95 percent of the total intact EOC cells with SKOV3 showing the highest activity. CD117 positive populations range from 31 to 79 percent of the total intact EOC cells with Kuramochi showing the highest activity. CD133

positive populations range from 10 to 93 percent with a2780-luc showing the highest activity (Figure 9c). We classified cells as CSCs if they were positive for more than one CSC marker. Shown are the triple CSC marker positive and therefore true cancer stem cells. These CSC populations range from 2 to 70 percent of the total intact cell population of the EOC cell lines (Figure 9d). A2780-luc, COV318, and Kuramochi are all positive for aldehyde dehydrogenase activity shown by Aldefluor positive populations, ALDH1 activity could not be determined in the OVCAR8 because they were GFP positive and the Aldefluor is detected in the GFP channel (Figure 9e).

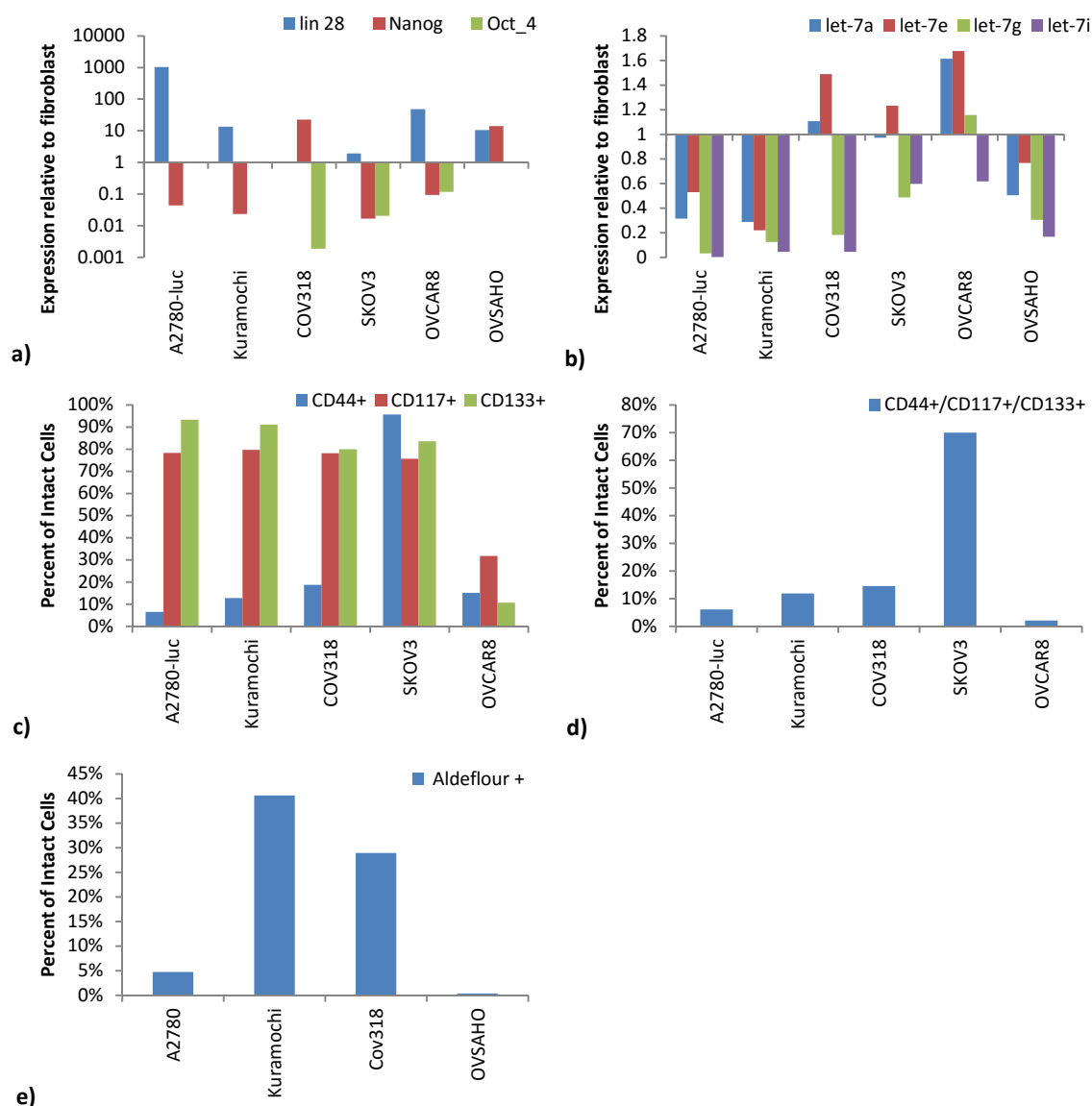


Figure 9. Cancer stem cell markers in epithelial ovarian cancer cell lines. a) qPCR for Lin28, Nanog and Oct4 expression in EOC cell lines. b) QPCR of Let-7 family members. c) Flow cytometry percent positive cells for CD44, CD117, and CD133. d) CD44, CD117, CD133 triple positive population of EOC cell lines. e) Aldefluor positive populations of EOC cell lines.

In the cancer stem cell population, it was observed that cells in the triple positive CD44/CD117/CD133 population were also double positive for N-



cadherin and E-cadherin (Figure 10a). This triple positive CSC population is 85 to 100 percent double positive for N-cadherin and E-cadherin (Figure 10b). The CD44, CD117, CD133, N-cadherin, and E-cadherin positive population makes up a small portion of the intact cells for most of the cell lines, ranging from 2 to 14 percent, but SKOV3 stands out as having a high population of these cells at 60 percent (Figure 10c).

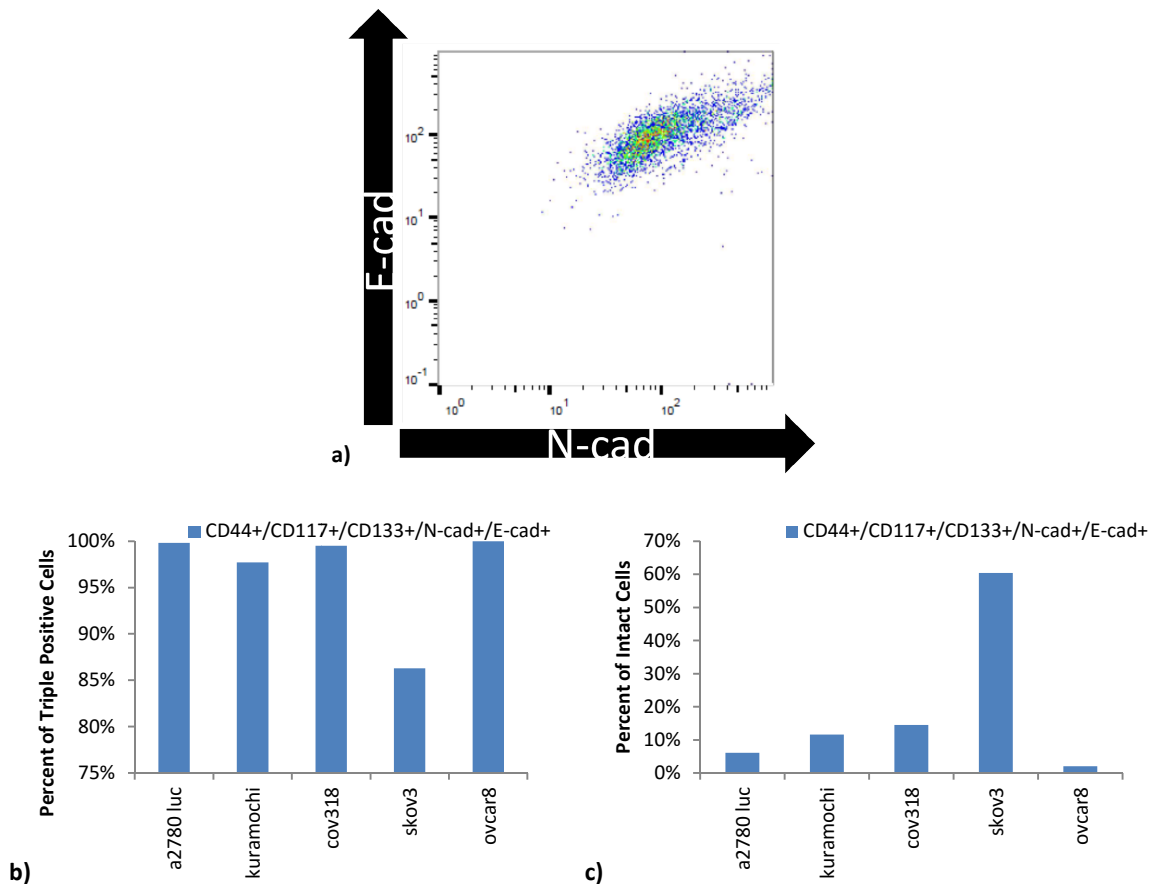


Figure 10. Cancer stem cells and epithelial mesenchymal transition. a) CD44, CD117, CD133 triple positive CSCs flow cytometry plot for N-cadherin and E-cadherin. b) Triple positive CSCs are 85 to 99% double positive for N-cadherin

and E-cadherin. c) CSC and N-cadherin/E-cadherin double positive cells out of entire intact population.

### 3.1.2 Metastatic Potential of Epithelial Ovarian Cancer Cell Lines

It was observed that only two cell lines show high activity in the scratch assay, defined as higher than normal fibroblasts, showing they have high motility: SKOV3, and OVCAR8 (Figure 11a). Scratch assay could not be performed on Kuramochi, OVSAHO or COV318 as when the scratch is performed on confluent plates the cells remove as a sheet instead of leaving the wound behind. In the soft agar assay showing anchorage independent growth the A2780-luc, OVCAR8 and SKOV3 all showed high ability to grow independent colonies (Figure 11b).

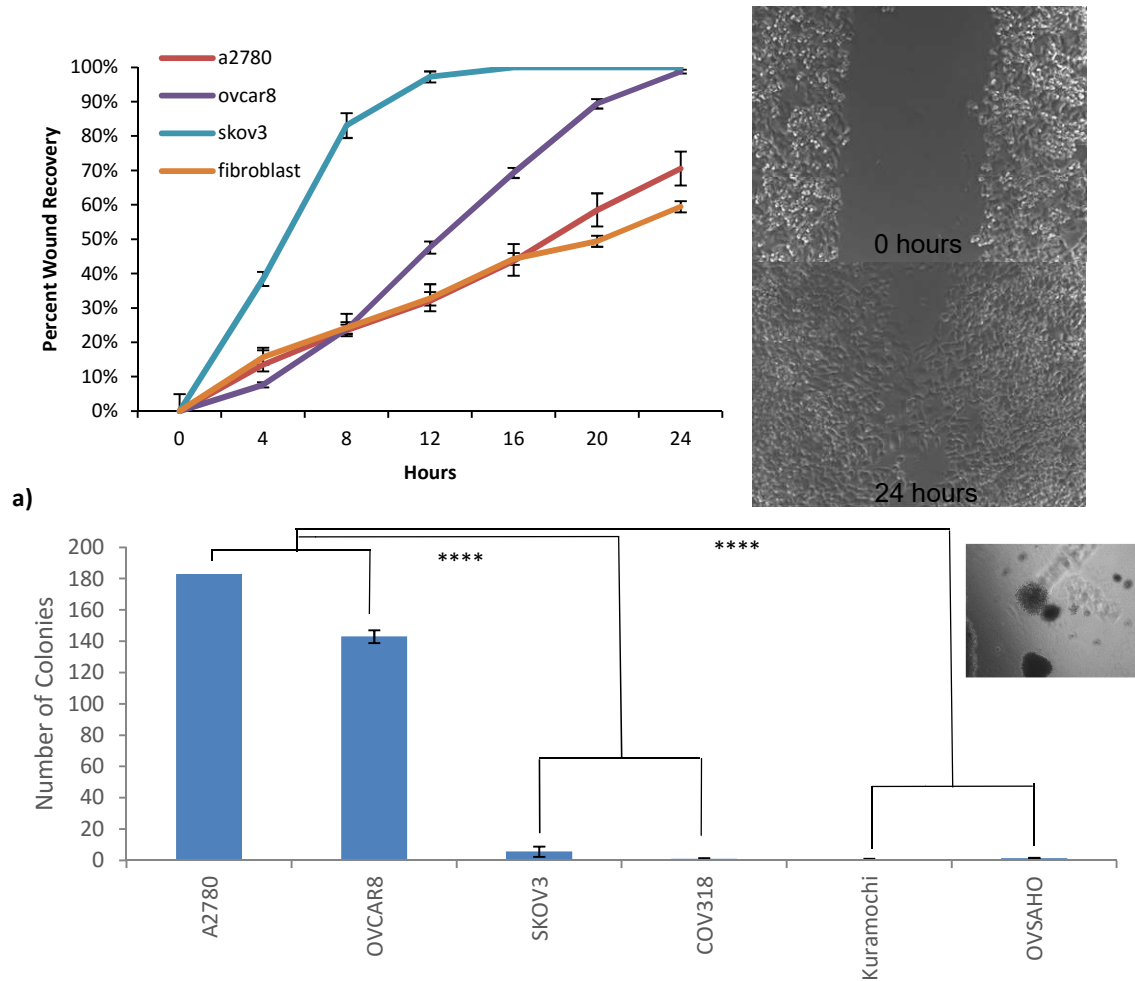


Figure 11. Metastatic potential assays of epithelial ovarian cancer. a) Scratch assay percentage wound healing over time with representative images of 0 and 24 hours of a wound. b) Soft agar assay colonies formed by each EOC cell line with representative image of colonies.

### 3.2 Aim 2: The Effect of Snail Knockdown on Epithelial Mesenchymal Transition status, Cancer Stem Cell makeup, and metastatic potential of an Epithelial Ovarian Cancer Cell Line OVCAR8

#### 3.2.1 Confirmation of Snail Knockdown

Snail knockdown was done virally and was tested with qPCR to confirm Snail was knocked down (Figure 12a). With shSnail, as the pluripotency marker

Nanog decreases let-7 miRNA levels increase (Figure 12a). This decrease in Nanog and increase in let-7 shows the shSnail exhibits less stemness than shControl. OVCAR8 shControl and shSnail showed no noticeable morphological changes (Figure 12b).

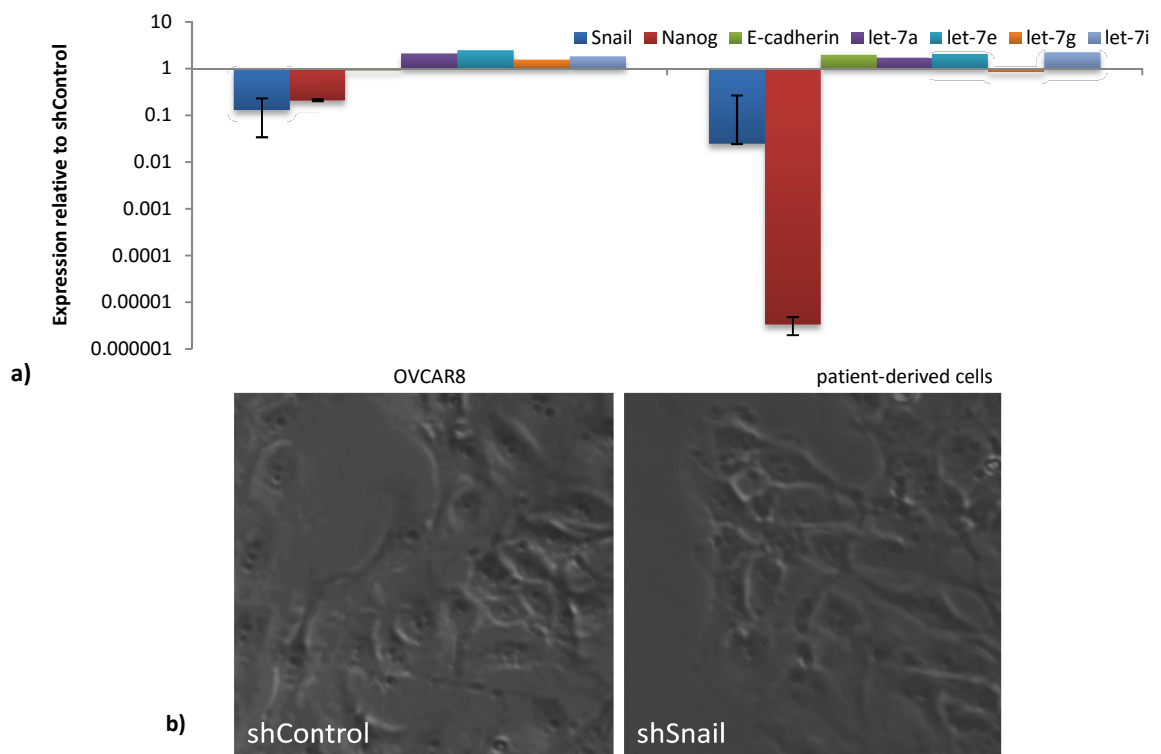


Figure 12. Confirmation of Snail knockdown and let-7 expression in shSnail. a) qPCR of Snail, Nanog, E-cadherin, and multiple let-7 miRNAs. b) Phase contrast bright field microscopy images of shControl and shSnail OVCAR8 cell lines.

### 3.2.2 Epithelial Mesenchymal Transition Status and Cancer Stem Cell Makeup in Snail Knockdown Model

The relative level of N-cadherin mRNA expression did not decrease in shSnail as expected; instead the expression increased (Figure 13a). shSnail did however decrease E-cadherin expression. The pathways leading to the mRNA expression of these two cadherins may not behave in cancerous cells as they do in normal cells. On a protein level, as percent of the total intact cell population, only very minor changes were detected in the shSnail OVCAR8 as compared to shControl. E-cadherin activity change was very low, 1.1x shControl. N-cadherin positive cells decreased only slightly to 0.98x shControl. N-cadherin/E-cadherin double positive cell populations did slightly increase with shSnail by 1.08x shControl (Figure 13b).

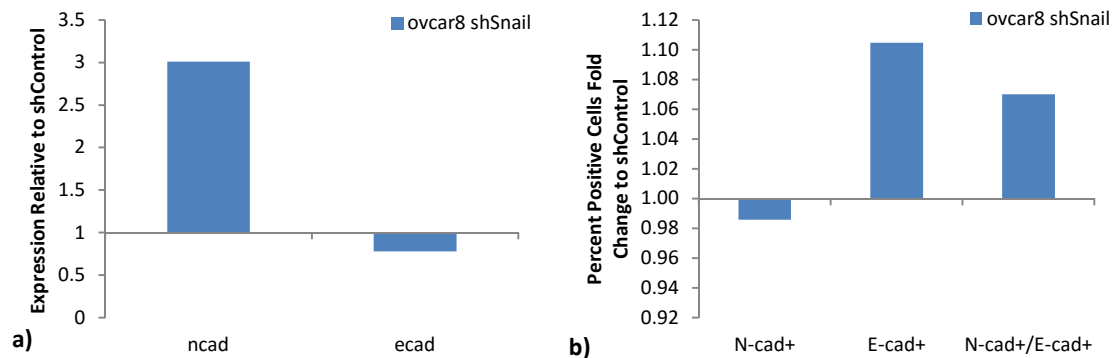


Figure 13. Epithelial mesenchymal transition markers in Snail knockdown model. a) qPCR for Snail, N-cadherin, and E-cadherin expression in shSnail EOC. b) Flow cytometry percent positive cells for E-cadherin, N-cadherin, and E-and N-cadherin double positive cells in shSnail EOC.

In OVCAR8 shSnail pluripotency mRNA markers Lin28, Nanog, and Oct4 all decreased (Figure 14a). CD133 positive cell population was extremely low in both shControl and shSnail, dramatically lower than the levels found in parental OVCAR8. The population of CD133 positive cells went from about 11% in the parental OVCAR8 (Figure 9c) to almost 0% in the virally treated cells (Figure 14b). Cancer stem cell marker CD44 positive population was decreased by over half in OVCAR8 shSnail (Figure 14c). Percentage of CD117 positive cell populations increased in OVCAR8 shSnail (Figure 14b). There were no triple positive CSC populations of cells detected in the shSnail model due to the loss of CD133.

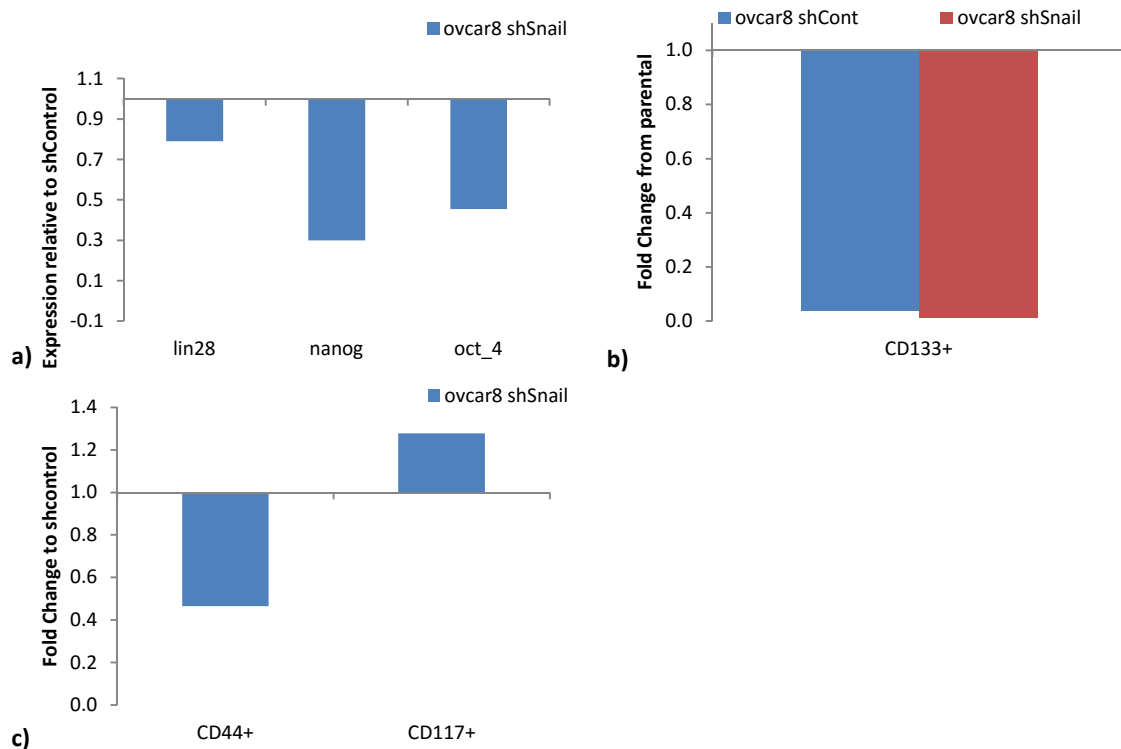


Figure 14. Cancer stem cell markers in Snail knockdown model. a) qPCR for Lin28, Nanog, and Oct4 expression in shSnail EOC. b) Flow cytometry CD133 activity in the virally transduced lines compared to the parental line. c) Flow cytometry percent positive cells for CD44, and CD117 in shSnail EOC normalized to shControl.

### 3.2.3 Metastatic Potential in Snail Knockdown Model

In OVCAR8, shSnail did not have a significant change in wound healing ability as compared to shControl. All virally treated cell lines were less able to colonize in anchorage independent growth compared to non virally treated cells. None of the virally treated pairs showed a significant difference in growth between the shControl and shSnail.

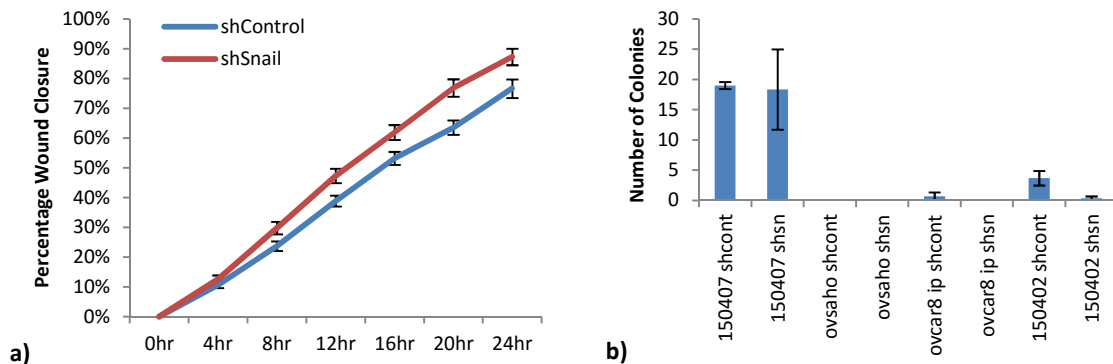


Figure 15. Metastatic potential assays of Snail knockdown epithelial ovarian cancer. a) Scratch assay percentage wound healing over time. b) Soft agar assay colonies formed by a variety of shSnail EOC cells.

### 3.2.4 Orthotopic Xenograft of Snail Knockdown OVCAR8

Snail knockdown showed a trend of a decrease in primary and metastatic tumor burden when compared to control in weight of tumor at harvest time (Figure 16a). Live imaging of the mice allowed the analysis of tumor growth in the live mice (Figure 16b). The analysis of the weekly mouse images did not show a difference in the primary growth of tumors with shSnail. This analysis did show a decrease in metastatic growth with a significant decrease in growth at day 43.



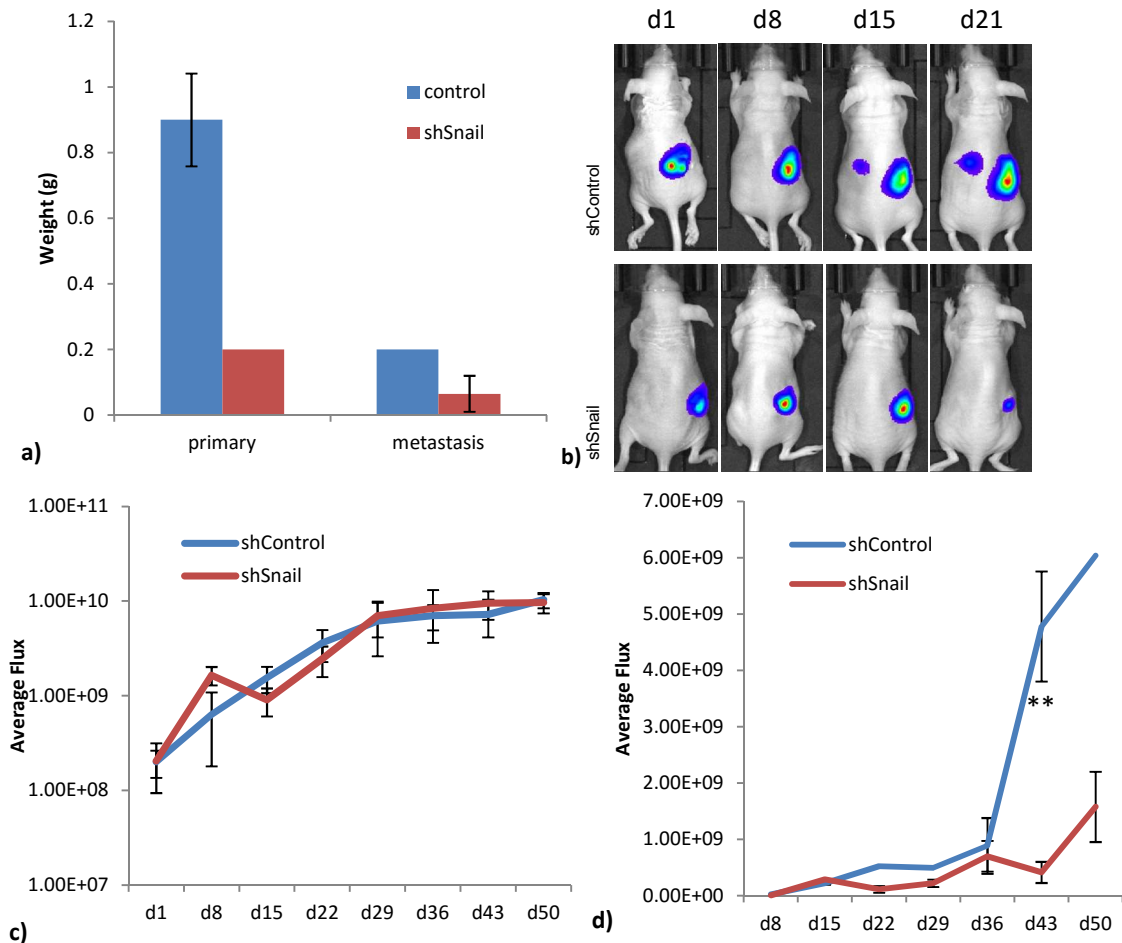


Figure 16. Xenograft model of Snail knockdown epithelial ovarian cancer. a) Representative IVIS images of shControl and shSnail tumors in mice. b) Weight of primary and metastatic tumors upon harvest. c) Fold increase from day 1 for primary ovarian tumor based on flux in IVIS images. d) Average flux of metastatic tumors in xenograft model.

## CHAPTER FOUR

### DISCUSSION

#### Epithelial Mesenchymal Transition and Cancer Stem Cells in Epithelial Ovarian Cancer

During a normal EMT event a cadherin switch from N-cadherin to E-cadherin occurs. E-cadherin transcription is down regulated and the competition between E- and N-cadherin for p120-catenin will increase N-cadherin activity and cause the endocytosis and degradation of E-cadherin<sup>25</sup>. Based on the high presence of N-cadherin/E-cadherin double positive cells in the EOC cell lines (Figure 8b) there could be changes in signaling leading to E-cadherin degradation with EMT events in cancer. Misregulation of the balance between p120 complexes at apical and basolateral cell-cell contact areas<sup>26</sup> could contribute to a faulty cadherin switch. The hybrid epithelial/mesenchymal state represents aberrant EMT and has been observed in cancer<sup>27</sup>. This would explain why the cell lines in this experiment showed a continuum of epithelial to mesenchymal behavior rather than remaining on one end of the spectrum or the other.

EOC lines have been evaluated as to their genomic similarity to patient samples<sup>28</sup>, growth characteristics, xenograft-forming ability<sup>29</sup>, genomic alterations, expression of markers, drug resistance, and in vitro behavior<sup>30</sup>. A few cell lines (OVSAHO, Kuramochi, COV318, OVCAR8) stood out as good examples of EOC based on previously published data<sup>28-30</sup>, therefore SKOV3 and

A2780 lines were eliminated from use after the initial characterization was complete. Kuramochi and OVSAHO stood out as the most epithelial lines when all data was combined and COV318 stood out as most mesenchymal. Notably, OVSAHO and Kuramochi were previously shown to poorly form xenografts<sup>30</sup>. OVCAR8 was shown to reliably and quickly form xenografts and ascites<sup>29</sup>. All three of these lines also contained CSCs at detectable but variable levels. OVCAR8 stood out as having a more hybrid phenotype between epithelial and mesenchymal states, a low to moderate level of CSCs, and high activity in metastatic potential assays; therefore, this line was chosen for the Snail knockdown model. Snail was detectable at levels above that in the mesenchymal fibroblasts used for normalization in all lines. Let-7 expression was observed to be lower than fibroblasts for most of the family members assessed. Notably, lines with lowest let-7 expression were observed to express higher levels of Lin28. This is consistent with decreased let-7 as a marker for CSC, but we have not tested whether the decreased let-7 levels are cause or effect of Lin28 expression.

EOC cell populations positive for CD44, CD117, and CD133 were classified as true cancer stem cells. Functional tests to prove this assertion will be done in the future. Cells positive for each of these markers individually have been classified as CSCs in other publications<sup>13,21,31</sup> however individually or in certain pairings these markers can be detected in progenitor cancer cells and not only in CSC<sup>13</sup>. We show that these triple positive cancer stem cells are the same

cells which are double positive for E-cadherin and N-cadherin. Therefore, the process that causes a cell to become a CSC may be the pathway both turning N-cadherin activity on and causing a loss of E-cadherin degradation that normally takes place in an EMT event. Identifying this CSC EMT positive subset of cells may be an important diagnostic and prognostic tool in the clinic. The ability to identify this subset could also be helpful in identifying best possible treatment plans for patients.

#### Epithelial Mesenchymal Transition and Cancer Stem Cells in Snail Knockdown Model of Epithelial Ovarian Cancer

In the shSnail model on a mRNA level the N-cadherin expression did not decrease, and the E-cadherin expression did not increase as expected. Instead the N-cadherin expression increased and the E-cadherin expression decreased (Figure 13a). On a protein level the percentage of cells positive for N-cadherin did decrease very slightly and the percentage of E-cadherin positive cells did slightly increase (Figure 13b). shSnail did decrease pluripotency mRNA expression for Lin28, Nanog, and Oct4. shSnail did not show a consistent loss of CSC surface markers; the CD44 positive population decreased as the CD117 population increased compared with shControl. CD133 activity decreased to almost nothing in both the virally delivered shControl and shSnail. Therefore, there were no triple positive CSC populations in the viral shRNA model. Taken together, we conclude that CD133, which has no published known function, may be involved in or is sensitive to the viral response of the cell in some way.

In the metastatic potential for the viral shRNA cell lines we did not determine there to be a difference in the metastatic potential between the shControl and the shSnail. In the scratch assay if there was a difference in the motility between shControl and shSnail we may not have been able to determine a difference due to differing proliferation rates of the cells lines. In both the cell line and viral shRNA line characterizations the motility in the scratch assay may have in part been due to the proliferation of the cells; for this reason, in the future we can inhibit the proliferation of cells with the use of mitomycin c treatment during the scratch assay.

In a xenograft model shSnail shows a trend of decreasing tumor burden for both primary and metastatic tumor burden as measured by weight of tumor burden at final harvest. A statistically significant difference was seen in the growth of the metastatic tumors by *in vivo* imaging analysis of live mice with metastatic growth in shSnail at day 43, as compared to shControl. Although Snail knockdown did not show all the anticipated responses *in vitro* Snail may still be a viable target in decreasing metastasis in cancer.

In the future we plan to use a different model to inhibit Snail activity in ovarian cancer, small inhibitory RNA (siRNA). In this study it became clear that the viral treatment of the ovarian cancer cells had some effect on the CSC and EMT makeup of the cell populations when comparing Figures 8 and 9 to raw population numbers in the sh model. The findings of the sh model are still valid

as the shSnail is compared to a shControl that was treated with the same viral treatment. This viral response would be avoided with the use of a siRNA.

## REFERENCES

1. Lamouille S, Xu J, Derynck R. Molecular mechanisms of epithelial-mesenchymal transition. *Nat Rev Mol Cell Biol* 2014;15(3):178-96.
2. Acloque H, Adams MS, Fishwick K, Bronner-Fraser M, Nieto MA. Epithelial-mesenchymal transitions: the importance of changing cell state in development and disease. *J Clin Invest* 2009;119(6):1438-49.
3. Cano A, Pérez-Moreno MA, Rodrigo I, Locascio A, Blanco MJ, del Barrio MG, Portillo F, Nieto MA. The transcription factor snail controls epithelial-mesenchymal transitions by repressing E-cadherin expression. *Nat Cell Biol* 2000;2(2):76-83.
4. Maeda M, Johnson KR, Wheelock MJ. Cadherin switching: essential for behavioral but not morphological changes during an epithelium-to-mesenchyme transition. *J Cell Sci* 2005;118(Pt 5):873-87.
5. Kurrey NK, Jalgaonkar SP, Joglekar AV, Ghanate AD, Chaskar PD, Doiphode RY, Bapat SA. Snail and slug mediate radioresistance and chemoresistance by antagonizing p53-mediated apoptosis and acquiring a stem-like phenotype in ovarian cancer cells. *Stem Cells* 2009;27(9):2059-68.
6. Zheng X, Carstens JL, Kim J, Scheible M, Kaye J, Sugimoto H, Wu CC, LeBleu VS, Kalluri R. Epithelial-to-mesenchymal transition is dispensable for metastasis but induces chemoresistance in pancreatic cancer. *Nature* 2015;527(7579):525-30.
7. Siegel R, Ma J, Zou Z, Jemal A. Cancer statistics, 2014. *CA Cancer J Clin* 2014;64(1):9-29.
8. Jemal A, Bray F, Center MM, Ferlay J, Ward E, Forman D. Global cancer statistics. *CA Cancer J Clin* 2011;61(2):69-90.
9. Karst AM, Drapkin R. Ovarian cancer pathogenesis: a model in evolution. *J Oncol* 2010;2010:932371.
10. Lengyel E. Ovarian cancer development and metastasis. *Am J Pathol* 2010;177(3):1053-64.
11. Ushijima K. Treatment for recurrent ovarian cancer-at first relapse. *J Oncol* 2010;2010:497429.
12. Markman M, Webster K, Zanotti K, Rohl J, Belinson J. Use of tamoxifen in asymptomatic patients with recurrent small-volume ovarian cancer. *Gynecol Oncol* 2004;93(2):390-3.
13. Burgos-Ojeda D, Rueda BR, Buckanovich RJ. Ovarian cancer stem cell markers: prognostic and therapeutic implications. *Cancer Lett* 2012;322(1):1-7.
14. Mitra A, Mishra L, Li S. EMT, CTCs and CSCs in tumor relapse and drug-resistance. *Oncotarget* 2015;6(13):10697-711.
15. Ojha R, Bhattacharyya S, Singh SK. Autophagy in Cancer Stem Cells: A Potential Link Between Chemoresistance, Recurrence, and Metastasis. *Biores Open Access* 2015;4(1):97-108.

16. Silva IA, Bai S, McLean K, Yang K, Griffith K, Thomas D, Ginestier C, Johnston C, Kueck A, Reynolds RK and others. Aldehyde dehydrogenase in combination with CD133 defines angiogenic ovarian cancer stem cells that portend poor patient survival. *Cancer Res* 2011;71(11):3991-4001.
17. Ayub TH, Keyver-Paik MD, Debald M, Rostamzadeh B, Thiesler T, Schröder L, Barchet W, Abramian A, Kaiser C, Kristiansen G and others. Accumulation of ALDH1-positive cells after neoadjuvant chemotherapy predicts treatment resistance and prognosticates poor outcome in ovarian cancer. *Oncotarget* 2015;6(18):16437-48.
18. Beck B, Blanpain C. Unravelling cancer stem cell potential. *Nat Rev Cancer* 2013;13(10):727-38.
19. Yamanaka S, Takahashi K. [Induction of pluripotent stem cells from mouse fibroblast cultures]. *Tanpakushitsu Kakusan Koso* 2006;51(15):2346-51.
20. Choi SA, Kim SK, Lee JY, Wang KC, Lee C, Phi JH. LIN28B is highly expressed in atypical teratoid/rhabdoid tumor (AT/RT) and suppressed through the restoration of SMARCB1. *Cancer Cell Int* 2016;16:32.
21. Foster R, Buckanovich RJ, Rueda BR. Ovarian cancer stem cells: working towards the root of stemness. *Cancer Lett* 2013;338(1):147-57.
22. Unternaehrer JJ, Zhao R, Kim K, Cesana M, Powers JT, Ratanasirintrao S, Onder T, Shibue T, Weinberg RA, Daley GQ. The epithelial-mesenchymal transition factor SNAIL paradoxically enhances reprogramming. *Stem Cell Reports* 2014;3(5):691-8.
23. Boyerinas B, Park SM, Shomron N, Hedegaard MM, Vinther J, Andersen JS, Feig C, Xu J, Burge CB, Peter ME. Identification of let-7-regulated oncofetal genes. *Cancer Res* 2008;68(8):2587-91.
24. Nimmo RA, Slack FJ. An elegant miRror: microRNAs in stem cells, developmental timing and cancer. *Chromosoma* 2009;118(4):405-18.
25. Wheelock MJ, Shintani Y, Maeda M, Fukumoto Y, Johnson KR. Cadherin switching. *J Cell Sci* 2008;121(Pt 6):727-35.
26. Kourtidis A, Ngok SP, Pulimeno P, Feathers RW, Carpio LR, Baker TR, Carr JM, Yan IK, Borges S, Perez EA and others. Distinct E-cadherin-based complexes regulate cell behaviour through miRNA processing or Src and p120 catenin activity. *Nat Cell Biol* 2015;17(9):1145-57.
27. Lu M, Jolly MK, Levine H, Onuchic JN, Ben-Jacob E. MicroRNA-based regulation of epithelial-hybrid-mesenchymal fate determination. *Proc Natl Acad Sci U S A* 2013;110(45):18144-9.
28. Domcke S, Sinha R, Levine DA, Sander C, Schultz N. Evaluating cell lines as tumour models by comparison of genomic profiles. *Nat Commun* 2013;4:2126.
29. Mitra AK, Davis DA, Tomar S, Roy L, Gurler H, Xie J, Lantvit DD, Cardenas H, Fang F, Liu Y and others. In vivo tumor growth of high-grade serous ovarian cancer cell lines. *Gynecol Oncol* 2015;138(2):372-7.



30. Elias KM, Emori MM, Papp E, MacDuffie E, Konecny GE, Velculescu VE, Drapkin R. Beyond genomics: critical evaluation of cell line utility for ovarian cancer research. *Gynecol Oncol* 2015;139(1):97-103.
31. Andrews TE, Wang D, Harki DA. Cell surface markers of cancer stem cells: diagnostic macromolecules and targets for drug delivery. *Drug Deliv Transl Res* 2013;3(2):121-42.